Laura R Rich[1] & Angus M Brown[1,2]

Fibre sub-type specific conduction reveals metabolic function in mouse sciatic nerve

[1] School of Life Sciences

University of Nottingham

Nottingham, NG7 2UH

UK

[2] Department of Neurology

School of Medicine

University of Washington,

Seattle, WA 98195

USA

Corresponding author

Dr Angus M Brown

School of Life Sciences

University of Nottingham

Nottingham, NG7 2UH

UK

Email: ambrown@nottingham.a.cuk

Phone: 0115 823 0173

Running title: Simultaneous recording of sciatic nerve A and C fibre CAPs

I graduated with a 1st class degree in Neuroscience from the University of Nottingham and proceeded to an M.Res., graduating with a distinction; the data from which is included in this paper. I am currently in my 1st year of a Ph.D. at Nottingham and interested in the role of glial cells in nervous system metabolic cell signaling. My career highlight is seeing my first research paper published in the prestigious Journal of Physiology and I hope to continue this career path to become an academic investigating the role of glial cells.

Key Points

- We have developed an improved method that enables simultaneous recording of stimulus evoked compound action potentials from large myelinated A fibres and small unmyelinated C fibres in mouse sciatic nerves.

- Investigations into the ability of fructose to support conduction in sciatic nerve revealed a novel glia-to-axon metabolic pathway in which fructose is converted in Schwann cells to lactate for subsequent shuttling to A fibres. The C fibres most likely directly take up and metabolise fructose.

- These differences are indicative of fibre sub-type specific metabolic profiles.

- These results demonstrate that the physiological insights provided by the method can be applied to investigations of peripheral nerve, with a view to understanding the metabolic disruptions that underlie diabetic neuropathy.

Abstract

The stimulus evoked compound action potential (CAP), recorded using suction electrodes, provides an index of the relative number of conducting axons within a nerve trunk. As such the CAP has been used to elucidate the diverse mechanisms of injury resulting from a variety of metabolic insults to central nervous white matter, whilst also providing a model with which to assess the benefits of clinically relevant neuro-protective strategies. In addition the technique lends itself to the study of metabolic cell-to-cell signalling that occurs between glial cells and neurones, and to exploring the ability of non-glucose substrates to support axon conduction. Although peripheral nerves are sensitive to metabolic insult and are susceptible to diabetic neuropathy, there is a lack of fundamental information regarding peripheral nerve metabolism. A confounding factor in such studies is the extended duration demanded by the experimental protocol, requiring stable recording for periods of many hours. We describe a method that allows us to record simultaneously the stimulus evoked CAPs from A and C fibres from mouse sciatic nerve, and demonstrate its utility as applied to

investigations into fibre sub-type substrate use. Our results suggest that C fibres directly take up and metabolise fructose, whereas A fibre conduction is supported by fructose-derived lactate, implying there exist unique metabolic profiles in neighbouring fibre sub-types present within the same nerve trunk.

Abbreviations

CAP   compound action potential

CIN   cinnemate

MON   mouse optic nerve

RON   rodent optic nerve

aCSF   artificial cerebrospinal fluid

ms   millisecond

Hz   Hertz

mM   milliMolar

Introduction

The area under the stimulus evoked compound action potential (CAP) recorded from isolated nerve trunks is indicative of the number of conducting axons (Cummins *et al.*, 1979), a phenomenon that has been used advantageously in investigations of injury mechanisms to central white matter, where the ratio of post- to pre-insult CAP area offers an index of injury, against which neuroprotective

strategies can be compared. The rodent optic nerve (RON), a central white matter tract, devoid of synapses and cell bodies, is cylindrical in shape and thus lends itself well to the recording of CAPs with suction electrodes (Stys *et al.*, 1991). The RON model has been used to investigate the mechanisms of anoxic (Stys *et al.*, 1992; Baltan Tekkök *et al.*, 2003; Allen *et al.*, 2005), aglycemic (Brown *et al.*, 2001a) and ischemic injury (Garthwaite *et al.*, 1999; Baltan *et al.*, 2008; Salter & Fern, 2008; Alix & Fern, 2009), as well as the roles of central glycogen (Brown *et al.*, 2003; Brown *et al.*, 2004), the ability of non-glucose substrates to support axon conduction (Brown *et al.*, 2001b), and the burgeoning area of glia-to-neurone metabolic signalling (Brown *et al.*, 2004; Brown *et al.*, 2005; Harris & Attwell, 2012).

Central tissue is more sensitive to acute oxygen and/or glucose deprivation than peripheral tissue (Devuyst & Bogousslavsky, 1999), and the consequences far more severe (Dirnagl *et al.*, 1999), with the result that such acute shortfalls in systemic energy supply would likely prove fatal before any peripheral nerve pathology was apparent, hence developing effective neuro-protective strategies targeted at central tissue is the primary clinical goal. However, peripheral nerves are affected by disturbed energy metabolism (Nave, 2010) with chronic hypoglycemia causing axon loss (Mohseni, 2001; Ozaki *et al.*, 2010). In the initial stages of diabetes small, unmyelinated peripheral axons suffer as a consequence of the prevailing hyperglycemia that ultimately proceeds to neuropathy (Tomlinson & Gardiner, 2008). Equivalent studies to those described above in the RON require extended recording periods. For example, whereas the mouse optic nerve (MON) CAP fails after 20 minutes of aglycemia and is abolished by 30 minutes (Brown *et al.*, 2003), the A fibre CAP of sciatic nerve persists for up to 90 minutes in aglycemic conditions with loss of the CAP complete after 3 to 4 hours, where, in the absence of exogenously applied substrate, Schwann cell glycogen is broken down to lactate, which is shuttled to the large myelinated A fibres to support conduction; the unmyelinated C fibres do not benefit from the presence of glycogen (Brown *et al.*, 2012). Although there are several studies relating to metabolism of sciatic nerve A fibres (Stecker & Stevenson, 2014; Stecker & Stevenson, 2015), there is a complete lack of equivalent C fibre studies, no doubt due to the very small amplitude of the

response, and the difficulty in achieving robust, reliable recordings. This limits basic understanding of C fibre metabolism, hampering insights into the metabolic disturbances that precede small fibre diabetic neuropathy.

The purpose of this paper is to describe an improved method that enables recording of stimulus evoked CAPs from mouse sciatic nerve A and C fibres simultaneously for extended durations, with a view to enhancing our understanding of peripheral nerve metabolism. With this goal in mind we proceeded with experiments to define the role of fructose as a substrate in sciatic nerve for the following reasons: (1) our method is ideal at revealing any differences in the fibre sub-type response to fructose, (2) fructose, created from glucose by the polyol pathway in Schwann cells (Champe & Harvey, 2008), may act as an endogenously created metabolic substrate, (3) fibre sub-type differences related to the efficacy of fructose as a substrate have been previously described in mouse optic nerve (Meakin *et al.*, 2007), and (4) there is evidence that fructose is converted to lactate in the hippocampus (Izumi & Zorumski, 2009), an intriguing parallel with the ability of glycogen-derived lactate to selectively support A fibres. We show that in the sciatic nerve C fibres appear to directly take up and metabolise fructose, whereas the benefit A fibres obtain from fructose is mediated by Schwann cell derived lactate. A preliminary account of this work has been presented to The Physiological Society in abstract form (Brown & Rich, 2017).

Methods and Materials

Ethical Approval

All experiments were approved by the University of Nottingham Animal Care and Ethics Committee, were carried out in accordance with the Animals (Scientific Procedures) Act 1986 under appropriate authority of establishment, project and personal licenses, and conform to the principles and regulations described in the Editorial by Grundy (Grundy, 2015).. Experiments were performed on male CD-1 mice (weight 28 - 35 g, corresponding to

30 - 45 days of age) purchased from Charles River Laboratories (Margate, Kent, CT9 4LT, UK). Mice were group housed with *ad libitum* access to food and water, and maintained at 22 - 23°C on a 12:12 hr light-dark cycle. Mice were killed by Schedule 1 cervical dislocation; death was confirmed by permanent cessation of the circulation. A total of 68 mice were used, with some nerves being used to provide data for more than one experimental condition, e.g. the data illustrated in Fig 4 was recorded prior to proceeding to the experiments shown in Fig 6. The majority of the nerves provided A and C fibre CAPs. In total 101 sciatic nerve recordings were made. The authors understand the ethical principles under which The Journal of Physiology operates and declare that our work complies with this animal ethics checklist.

Dissection of the mouse sciatic nerve

Adult male CD-1 mice were killed Schedule 1 methods (see above). There is no indication to suggest that the method of humane killing has any detrimental impact on the sciatic nerve. The mice were pinned prone on a corkboard, with dissecting pins inserted through each limb, the tail facing the dissector. The hind limbs were pinned at right angles to the body to optimise the ease of dissection. We strongly concur with the authors of a similar methodological study involving the vagus nerve, that it is the care with which the dissection is carried out rather than the speed that is the critical factor affecting viability of the preparation (Docherty *et al.*, 2005). We started dissection on the right side as this favoured the right-handed authors. Although each nerve takes about 5 minutes to remove, the 10-minute delay in removing the left nerve is insufficient to compromise its viability. An incision is made along the vertebrae starting at the neck with a size 23-scalpel blade, and continued distally for between 4 and 5 cm towards the tail. About 1 cm above the tail a further incision is made along the posterior right hind leg towards the foot. The skin is retracted and pinned to maximise exposure of the vertebrae and the muscle overlying the right hind leg. To expose the sciatic nerve an incision is made about half way down the back, through the muscle immediately to the right of the vertebrae and continued towards the tail. The incision is then directed along the posterior aspect of the right hind leg towards the foot. Gentle excision of overlying muscle exposes the sciatic nerve, which lies superior to this incision (Fig 1A). The nerve emerges from the spinal cord at L4 to 6, and proceeds caudally, prior to following the course of the leg at the sciatic notch. The sciatic nerve splits into separate cable like structures before dividing in the popliteal fossa into the sural, tibial and peroneal branches. Care is taken when dissecting at the sciatic notch, as there are numerous cutaneous branches that must be severed. Running the scalpel blade on either side of the nerve at the sciatic

notch liberates the nerve from particularly tough connective tissue adhesions and collateral cutaneous branches. A pair of forceps can then be passed underneath the nerve to remove any remaining lesions with neighbouring tissue, and careful retraction of the nerve from the muscle frees the tissue. The nerve is cut where it emerges from the vertebrae and gently pulled down towards the tail to return tension to the nerve, thereby making it easier to make the final cut in the leg and helping ensure the longest length of nerve possible is dissected. It is then cut distal to where it branches in the leg and gently transferred to the superfusion chamber. The nerves we recorded from were between 11 and 12 mm in length. The procedure for the left sciatic nerve is similar, although we have found it easier to rotate the corkboard by 180° so that the tail now faces away from the dissector. In this manner the right hand direction of incision along the left leg is preserved. We routinely use two identical set ups to record from both sciatic nerves, each providing an A and C fibre response. This efficiency is in accord with the National Centre for Replacement, Refinement and Reduction in Animal Experiments in the UK.

Superfusion chamber

The nerves were allowed to equilibrate in the interface superperfusion chamber (Medical Systems Corp, Greenvale, NY), for 10 to 15 minutes prior to recording. The nerves were maintained at 37°C and superfused with aCSF containing (in mmol/L): NaCl 126, KCl 3.0, $CaCl_2$ 2.0, $MgCl_2$ 2.0, NaH_2PO_4 1.2, $NaHCO_3$ 26 at a rate of about 2 ml min^{-1}. Control aCSF contained 10 mM glucose. The substrate in the aCSF can be omitted completely (substrate-free), or replaced with another, in order to study aglycemia or fructose metabolism, respectively. The chamber was continuously aerated by a humidified gas mixture of 95% O_2/5% CO_2. Suction electrodes back filled with substrate-free aCSF, to preclude creation of substrate-rich reservoir, were used for stimulation and recording. Prior to insertion into the suction electrodes the ends of the nerves were carefully trimmed with McPherson-Vannas scissors with 3 mm blades (14177: WPI, Sarasota, FL 34240, USA), as this was found to contribute to stable recordings. Nerves were gently introduced into the suction electrodes, such that orthodromic recordings were made (Fig 1B). The suction electrodes were manufactured as previously described (Stys *et al.*, 1991), where electrodes were fashioned from capillary glass and shaped with a Bunsen burner; trial and error melting of the tip of the glass produced electrodes of optimal diameter.

Electrophysiological recordings

The recordings of the stimulus evoked CAPs were controlled by proprietary software. A Grass S88 stimulator connected to two SIU5 isolation units in parallel was used to stimulate the nerve. The Grass S88 is capable of delivering paired pulses; the duration and amplitude of each can be independently controlled, as can the delay between the two pulses. In our previous publication on sciatic nerve only the A or C fibre CAP was recorded from each nerve (Brown *et al.*, 2012), but this new method offers an ideal opportunity to evoke simultaneously the A and C fibre CAPs from each sciatic nerve, which allows comparison of A and C fibre responses under identical experimental conditions. We were unable to distinguish the sub-groups of A fibre, thus the low threshold CAP we recorded was considered to comprise contributions of all A fibres. The sciatic nerve is composed of two distinct fibre sub-types. The large A fibres (up to 10 μm in diameter) are myelinated by Schwann cells, whereas the smaller (up to 1 μm in diameter), unmyelinated C fibres are enclosed in groups within Schwann cell cytoplasm into Remak bundles (Fig 2). Size and the presence of myelin confer upon each fibre sub-type a conduction velocity that is reflected in the profile of the stimulus evoked CAP. In addition, fibre size determines the stimulus threshold at which action potentials are evoked (Patton, 1982). The signal was amplified up to x1000 in AC mode by a Stanford Research Systems Preamplifier (SR560, Stanford Research Systems, Sunnyvale, CA) and filtered at 30 kHz and acquired at 20 kHz (Clampex 9.2, Molecular Devices, Wokingham, UK). The field potential generated by the stimulus artefact was recorded by a AgCl wire wrapped around the outside of the recording electrode, with a separate AgCl wire inserted into the lumen of the capillary glass to record the CAP. The CAP was obtained using the differential properties of the amplifier, where the artefact was eliminated by subtraction. Each CAP was recorded in this manner, thus the CAP represents the active response minus the passive stimulus artefact. In order to remove the remaining transient artefact (for details see Stys *et al.*, 1991) the nerve was crushed between forceps at the conclusion of each experiment, ensuring only the passive response was recorded. In post experimental processing the crushed response was subtracted from each CAP.

Lactate biosensors

Lactate and null biosensors were purchased from Sarissa Biomedical (Coventry, UK). In these experiments, however, the lactate signals were sufficiently large that subtraction of

the null signal did not meaningfully alter the lactate signal amplitude. The lactate biosensors (25 μm in diameter and 500 μm in length) were pressed against the sciatic nerve, to record [lac] release from the nerve. Experimental recordings began after an equilibration period of up to an hour. At the beginning and end of all experiments, lactate biosensors were calibrated using lactate concentrations of 10 μM and 100 μM. Results were considered valid only if the before and after calibrations deviated by no more than 10 %.

Transmission Electron microscopy (TEM)

Sciatic nerves were dissected as described above, laid out on cardboard and then immediately fixed in 2% glutaraldehyde and 2% paraformaldehyde in 0.2 M phosphate buffer overnight and post-fixed in 1% osmium tetroxide for 30 minutes. They were dehydrated in a graded ethanol series and embedded in Transmit low viscosity resin (TAAB). Semi thin sections were cut at 0.5 μm, stained with toluidine blue and photographed using a Leica DM400B light microscope with colour digital camera and Openlab darkroom software. Ultrathin sections (70 - 90 nm) were prepared using a Reichert-Jung Ultracut E ultramicrotome and mounted on 100 hexagonal copper grids. They were contrasted using Uranyl acetate and Lead Citrate and viewed using a JEOL 1010 TEM operated at 80 kV with digital image acquisition.

Data Analysis

Stimulus evoked CAPs were digitized via a Digidata 1200 A/D board, recorded using PClamp 9.2 and analysed with Clampfit 9.2 (Molecular Devices, Wokingham, UK). The freely available WinWCP, part of John Dempster's Strathclyde Electrophysiology Software suite of programmes, allows equivalent acquisition and analysis (WinWCP). The duration of each episodic record was 60 ms to accommodate both A fibre and C fibre CAPs, respectively, which were evoked with a 30 μs rectangular pulse of up to 15 V, followed 20 ms later with a 30 μs pulse of up to 150 V, respectively. In order to visualise the C peak, which is sufficiently small to be obscured by background electrical noise, we used options available in the acquisition software to aid visibility. We opened a separate window in which the running average of the traces was superimposed on the individual traces, resulting in a clearly discernible, distinct peak. The duration of these experiments requires the ability to monitor

the A and C fibre CAP amplitudes over extended periods of time, and simply displaying overlapping traces is inadequate due to the limitations of identifying individual traces. We opened a separate viewing window that plots A fibre CAP peak amplitude as it is acquired, enabling us to monitor the A fibre CAP amplitude in real time over the course of the entire experiment: a similar procedure can be applied to the C fibre CAP. Nerves were stimulated at 1 Hz, with sixty traces averaged then recorded: the use of sequencing keys allowed us to automate continuous recording of the averaged CAPs. The C fibre CAP was measured as area, rather than amplitude as this better reflects the number of contributing axons (Patton, 1982). The ability of substrates to support conduction can be measured as the area under the normalised CAP over time, as illustrated by the shaded area in Fig 6A (GraphPad Prism 7). This conversion of raw data into a quantifiable measure of substrate efficacy provides a numerical basis for statistical analysis.

Statistical Analysis.

Descriptive statistics are expressed as the mean ± standard deviation and n refers to the number of nerves. An n value of between 3 and 6 was used for each condition in the experiments (see Figure Legends for details). The stimulus strength versus A and C fibre amplitude (Fig 4A) was fit with a Boltzmann sigmoidal curve of the form:

$$y = \frac{1}{1 + \exp^{\frac{V_{0.5}\text{-stim current}}{\text{slope}}}}$$

where $V_{0.5}$ indicates the stimulus current where the half maximal amplitude occurs and slope occurs at $V_{0.5}$. A modified version of this equation was used to measure the CAP area over time shown as the shaded area in Fig 6A. One-way ANOVA with Sidak post-tests were used to determine the significance of selected inter-group differences. All data were analysed with GraphPad Prism 7 (La Jolla, CA 92037, USA).

Results

CAPs recorded from mouse sciatic nerve

An example of CAPs recorded from sciatic nerve using a paired pulse protocol designed to selectively recruit the A and C fibres is shown in Fig 3A. The initial pulse (30 μs

duration, 15 V amplitude) recruited all the available A fibres, producing a monophasic profile that peaked within 0.5 ms of the stimulus. A second pulse (20 ms later, 30 μs duration, 130 V amplitude) produced a more complex profile. The large negatively going deflection lasted between 5 and 10 ms, and incorporates not only the artefact, but also includes the maximal A fibre response. The small C fibre CAP occurs between 13 and 18 ms after the stimulus and lasts about 7 ms. Depending upon recording conditions and the length of the nerve, the C fibre CAP can occur on the rising phase of the artefact necessitating its subtraction to ensure a stable baseline. The relatively small amplitude of the C fibre CAP produces an individual trace that is obscured by the ambient noise (Fig 3Bi) making distinguishing the CAP profile difficult. We have used signal averaging properties of the acquisition software to boost the signal to noise ratio by evoking the C fibre CAP every second, and displaying a running average of the traces, such that each trace is displayed as in Fig 3Bi, but superimposed on top of this trace, in a different colour, is the running average of the responses (Fig 3Bii), which optimises viewing. The stimulus artefacts can interfere with the A and C fibre peaks, and are removed post-acquisition in order to reveal the active response of the nerve uncontaminated by artefact (see Methods). The effects on both the A and C fibre CAPs, respectively, are illustrated in Fig 3C and Fig 3D, respectively.

Characteristics of the CAPs

The selective recruitment of the A and C fibres is shown in Fig 4A. The A fibres have a lower recruitment threshold (~5 V), with the maximal response reached between 10 and 15 V. In contrast the C fibres have a threshold of about 50 V, with the maximal response reached between 100 and 150 V. Thus, the stimulus required to maximally recruit all available A fibres is below that for C fibre recruitment. There is about a 50 to 100-fold difference in the maximum peak amplitude of the A and C CAPs (Fig 4B), which significantly contributes to the difficulty in recording the C fibre CAP. A double pulse protocol was used to investigate the relative refractory period of the A fibre CAP. The extended latency between introduction of substrate-free aCSF and failure of the A fibre CAP (Brown *et al.*, 2012) increases the recording duration of experiments investigating the ability of non-glucose substrates to support the CAPs. We sought ways of accelerating CAP failure by increasing tissue energy demand by imposing high frequency stimulus (Brown *et al.*, 2003). However, this procedure is accompanied by the risk of misinterpreting decreases in the A fibre CAP which are due to inactivation of the Na^+ channels rather than a real metabolic effect, thus we must first

determine the relative refractory period of the A fibre CAP. This was estimated using a double pulse protocol in which the 1st pulse evoked the maximum A fibre CAP, followed by a 2nd pulse of an equivalent magnitude at decreasing inter-pulse intervals to determine when the 2nd peak started to decrease, an indication that the Na^+ channels were not allowed sufficient time to recover from inactivation after the 1st pulse (Fig 4C). Plotting the ratio of the amplitude of the 2nd pulse relative to that evoked by the 1st pulse demonstrated that at inter-pulse intervals below 5 ms the amplitude of the CAP evoked by the 2nd pulse began to fail (Fig 4D), which equates to a frequency of 200 Hz. We imposed 50 Hz stimulus commensurate with introduction of substrate free aCSF. The A fibre CAP fell more rapidly in these conditions than when stimulated at 1 Hz. We have previously shown that imposing high frequency stimulus causes a depletion of glycogen in MON (Brown *et al.*, 2003), and presume that an equivalent process occurs in the sciatic nerve under conditions of imposed high frequency stimulus. Thus we are confident that the accelerated A fibre CAP failure we see when imposing 50 Hz stimulus (Fig 6A & D) is due entirely to stimulus induced exhaustion of glycogen supplies (Brown *et al.*, 2003), although it should be borne in mind that the processes that reduce the number of active channels rather than the kinetics of their inactivation will not be identified by this method.

Metabolic studies

Metabolic studies on the sciatic nerve in which the CAP is used as an index of conduction tend to require extended recording periods (Brown *et al.*, 2012; Stecker & Stevenson, 2015). We have successfully recorded A and C fibre CAPs, with no loss of amplitude, when incubated with control aCSF for over 8 hours, and even longer recordings of A fibre CAPs are possible (Stecker & Stevenson, 2015). Such extended durations lend themselves to experiments where the ability of non-glucose substrates to support conduction can be investigated. Sciatic nerves were exposed to 10 mM glucose while simultaneously recording the A and C fibre CAPs. On exposure to substrate free aCSF the C fibre CAP fell after about 30 minutes, followed after about 90 minutes by the A fibre CAP as previously reported (Brown *et al.*, 2012). Exposure to 10 mM fructose aCSF led to a rapid recovery of the C fibre CAP, but the A fibre CAP continued to fall to zero. The A fibre was rescued by introduction of control aCSF. Subsequent introduction of 10 mM fructose aCSF led to a rapid failure of the A fibre CAP, whilst the C fibre CAP was maintained (Fig 5).

Ability of fructose to maintain the CAP

The A fibre CAP was fully supported for 8 hours in 10 mM glucose and 20 mM fructose aCSF, but not in 5 mM or 10 mM fructose. The similarity in the latency to CAP failure between 5 mM or 10 mM fructose, and substrate free aCSF suggests that at these concentrations fructose offers no benefit to the A fibres. The C fibre CAP however was more robust when fructose was the sole exogenously supplied substrate, with 10 mM glucose and 20 mM fructose supporting the CAP for 8 hours, and 10 mM fructose and 5 mM fructose fully supporting the CAP for 5 to 6 hours before it slowly fell (Fig 6B and C). Imposing 50 Hz stimulus at the onset of introduction of substrate free aCSF, significantly accelerated A fibre CAP failure, the result of increased tissue energy demand exhausting glycogen reserves sooner (Fig 6A and C).

The disparity between 10 mM and 20 mM fructose support of the A fibre CAP was investigated for the following reasons. We have found in MON that 2 mM glucose supported the CAP. However depleting glycogen with brief exposure to substrate-free aCSF resulted in subsequent exposure to 2 mM glucose being incapable of supporting the CAP (Brown *et al.*, 2003). We used a similar strategy to see whether an equivalent scenario was occurring i.e. that in the presence of 10 mM fructose, glycogen was metabolised to support the A fibre CAP, but once the glycogen was depleted the fructose would be incapable of fully supporting the A fibre CAP (see Fig 5). We exposed the nerve to 2 hours of 10 mM glucose, 20 mM fructose or 10 mM fructose aCSF, then switched to substrate-free aCSF. The A fibre CAP began to fail rapidly in nerves pre-incubated in 10 mM fructose, but there was no significant difference in the latency to CAP failure when nerves were pre-incubated in 10 mM glucose or 20 mM fructose (Fig 7A and B).

Ability of fructose to recover the CAP

It must be appreciated that substituting glucose with fructose does not overcome the complication of glycogen present in the tissue supporting conduction in the nerve, thus clouding interpretations of the results; this was addressed in experiments where substrate-free aCSF was introduced in order to deplete glycogen, signalled by the onset of A fibre CAP failure. When the CAP had fallen to between 50 and 75 % of its baseline amplitude solutions of 10 mM glucose, 20 mM fructose or 10 mM fructose were introduced. 10 mM glucose and 20 mM fructose restored the CAP, although the CAP recovered quicker with 10 mM glucose,

whereas 10 mM fructose was unable to rescue the CAP, the contrast with glucose clearly illustrated when subsequent introduction of 10 mM glucose aCSF rapidly restored the CAP (Fig 8A, C and D). In the C fibres the CAP was equally restored in 10 mM glucose, 20 mM fructose or 10 mM fructose aCSF (Fig 8B, C and D).

Effect of blocking lactate uptake with cinnemate

In light of the role of glycogen in supporting the CAP in 10 mM fructose, and the trafficking of fructose to lactate reported in the hippocampus (Izumi & Zorumski, 2009), we used the compound cinnemate (200 µM) to interrupt lactate uptake into axons (Choi *et al.*, 2012), with a view to dissecting direct fructose uptake into axons, from fructose derived lactate production. The most likely source of lactate is the Schwann cell given the established ability of astrocytes to fulfil this function in the CNS (Pellerin *et al.*, 2007). Maintenance of CAPs in 10 mM glucose, 20 mM fructose or 10 mM fructose plus cinnemate showed clear differences between the A and C fibres. Only 10 mM glucose was able to fully support the A fibre CAP in the presence of cinnemate, with CAP failure occurring with 20 mM fructose or 10 mM fructose plus cinnemate (Fig 9A and C). However C fibre CAPs proved more robust, with failure occurring with 10 mM fructose plus cinnemate towards the end of the experimental time period (Fig 9B and D). As a further test of the phenomenon we carried out recovery experiments in the presence of cinnemate to block axonal uptake of lactate. Cinnemate had no effect on the ability of 10 mM glucose to recover the A fibre CAP (Fig 10A and D), but rendered 20 mM fructose unable to restore the CAP (Fig 10B and D). The stark contrast between 20 mM fructose and 10 mM glucose is illustrated, where 10 mM glucose plus cinnemate rapidly restores the CAP, but subsequent exposure to 20 mM fructose and cinnemate causes rapid CAP failure, indicating that lactate uptake into A fibre underlies the support provided by 20 mM fructose (Fig 10B). The ability of 10 mM glucose, 20 mM fructose and 10 mM fructose to restore the CAP in the C fibres was unaffected by cinnemate (Fig 10C and D).

Extracellular lactate measurements

We used lactate biosensors to explore extracellular lactate ([lac]) in sciatic nerve, since our results favour a fructose derived lactate flux that supports the A fibre CAP. A lactate dose response curve was constructed in the presence of various concentrations of

glucose ([glucose]), which showed saturation of the lactate signal above about 5 mM glucose (Fig 11A). The [lac] measured at the edge of the nerve is relatively low in nerves perfused with 10 mM glucose ($\sim$50 μM). Bathing the sciatic nerve in 20 mM fructose caused a fall in [lac] to a stable baseline value of between 15 and 20 μM, but when 10 mM fructose aCSF was perfused [lac] gradually fell towards zero (Fig 11B: see discussion). For this reason we were unable to construct a lactate dose response curve with fructose. To test the hypothesis that the delay in the recovery of the A fibre CAP in 20 mM fructose, relative to that of glucose, is due to delayed production of lactate in the presence of fructose, we bathed the nerves in substrate free aCSF until the CAP started to fall, while simultaneously recording [lac]. At the onset of aglycemia [lac] fell to zero as previously reported (Brown *et al.*, 2012). Introduction of 20 mM fructose aCSF resulted in a delayed increase in [lac], whose time course suggested that the A fibre CAP only starts to recover when the [lac] plateaus after introduction of fructose aCSF (Fig 11C). To further confirm this conversion of fructose to lactate we recorded a stable [lac] of 15 μM in nerves perfused with 20 mM fructose before subsequent addition of cinnemate, which resulted in a slow, steady increase in [lac] (Fig 11D) that reversed upon washout of cinnemate.

Discussion

The results described in this paper demonstrate that in mouse sciatic nerve both the A and C fibre CAPs are maintained with fructose as the sole exogenously applied substrate if delivered at a sufficiently high concentration. If the concentration of fructose is lowered however, only the C fibres continue to conduct. Whereas the C fibres appear to directly take up and metabolise fructose, the A fibre benefit from fructose is mediated by a Schwann cell-to-axon lactate shuttle. Our results suggest that there exist in the sciatic nerve two distinct metabolic profiles in neighbouring fibre sub-types.

Recording from in vitro sciatic nerve

The method we describe in this paper allows for the simultaneous, extended recordings of A and C fibre CAPs. We were prompted to develop this method based on our initial publication describing the effects of aglycemia on sciatic nerve A and C fibre CAPs,

which demonstrated clear inter-fibre differences, namely the shorter latency to C fibre CAP failure compared to A fibres, due to the presence of Schwann cell glycogen that is metabolised to lactate and shuttled to the A fibres (Brown *et al.*, 2012). Such metabolic distinctions between two fibre sub-types present in the same nerve trunk implied a previously unsuspected metabolic versatility and diversity. This observation is of particular interest since the unmyelinated C fibres, which do not benefit from glycogen, are more susceptible to diabetic injury than myelinated A fibres (Navarro *et al.*, 1989; Lacomis, 2002), suggesting a potential metabolic cause of small fibre diabetic neuropathy based on substrate availability and use.

The sciatic nerve A fibre CAP can survive for up to 2 hours in the absence of exogenously applied glucose, underlining the sluggish metabolic rate of peripheral nerve when compared to central white matter (Hothersall *et al.*, 1982), where the CAP would fail within 20 minutes under equivalent circumstances (Brown *et al.*, 2003; Brown *et al.*, 2005). As a consequence experiments designed to investigate the ability of non-glucose substrates to support conduction are inevitably of long duration, although A fibre CAP failure is accelerated if introduction of substrate-free aCSF is accompanied by imposition of 50 Hz stimulus, which we have previously shown as an effective means by which to deplete glycogen (Brown *et al.*, 2003; Brown *et al.*, 2005). We have identified the following confounding factors that impede the ability to successfully carry out such experiments: (i) stability of recordings, (ii) ability to visualise the A fibre CAP amplitude in real time, and (iii) ability of visualise the C fibre CAP profile and amplitude/area in real time. The differences in response of the A and C fibre CAPs to substrate-free aCSF convinced us of the merits of recording simultaneously the A and C fibre CAPs. The differences in threshold of the two fibre types precludes the opportunity to evoke both fibres with a single pulse, accordingly we used a Grass S88 stimulator to deliver paired pulses to the nerve. The large A fibres have a lower threshold than the C fibres, and a small (up to 15 V) pulse was used to recruit the A fibres. A delay of 20 ms separated this pulse from the 2nd pulse (up to 150 V) used to evoke the C fibres. The threshold for the C fibres is higher than that for the A fibres, thus the 1st pulse will have no effect on the C fibres. The latency between the stimulus used to evoke the C fibre CAP, which emerges 13 to 18 ms later, means that although the 150 V pulse will maximally recruit the A fibres, their response will not interfere with the slower conducting C fibres. This method allows us to make comparisons of conduction between the fibre sub-types under identical experimental conditions.

C fibre CAP profile

We have been unable to locate any publications illustrating recordings from unmyelinated C fibres from mouse sciatic nerve of equivalent duration to those illustrated in this paper. The primary model for electrophysiological examination of unmyelinated fibres has been the vagus nerve, which comprises 90% unmyelinated axons, where the preferred recording environment is either the sucrose (Gaumann *et al.*, 1992, 1994; Erne-Brand *et al.*, 1999; Dalle *et al.*, 2001; Jirounek *et al.*, 2002) or grease gap (Docherty *et al.*, 2005) techniques. The sucrose gap technique requires a very short conducting distance in order to minimise the temporal dispersion of action potential arrivals, thereby maximising the amplitude of the CAP (Velumian *et al.*, 2010). However, from a metabolic viewpoint, the vagus nerve is of limited translational relevance, as it is the sciatic nerve that is exquisitely sensitive to diabetes, with initial symptoms of neuropathy emanating from the distal sciatic nerve in the foot (Navarro *et al.*, 1989). The C fibre CAP profile, a discrete peak of about 7 ms duration, 13 to 18 ms after the stimulus, is indicative of a contributing axon population of limited diameter range. Since conduction velocity is proportional to the square root of axon diameter in unmyelinated axons (Rushton, 1951; Hodgkin, 1954; Waxman & Bennett, 1972), applying this relationship to our recordings in sciatic nerve of length 12 mm, results in an estimated axon diameter range of between 500 μm and 900 μm. We have not carried out an equivalent study to the one we conducted in MON, where we used TEM to construct axon diameter histograms (Allen *et al.*, 2006), but these estimated axon diameters match those illustrated in Fig 2. Considering the relationship between stimulus amplitude and amplitude of the evoked C fibre CAP as a cumulative distribution function relating stimulus intensity to axon threshold (Fig 4A), implies that the slope is indicative of the standard deviation of distribution. If we accept that the C fibres represent a homogeneous, unmyelinated axon population, then the principal variable that determines threshold is axon size. Since conduction velocity varies with axon size in a predictable manner, the relatively steep slope is reflected in the discrete C fibre CAP, whose profile is of a sufficient magnitude to make meaningful measurements.

Fructose metabolism

Fructose was one of the first non-glucose substrates shown to support *in vitro* brain

slices (Bernheim & Bernheim, 1941; Klein, 1944; McIlwain, 1953), and has since been shown to support both central grey matter (McIlwain & Bachelard, 1985; Izumi & Zorumski, 2009), white matter (Allen *et al.*, 2006; Meakin *et al.*, 2007) and sciatic nerve (Stecker & Stevenson, 2015). In the MON 10 mM fructose exhibits the intriguing property of supporting the smaller axons, but not the larger ones, due to selective distribution of the enzyme fructokinase (Meakin *et al.*, 2007), which has a high affinity and high capacity for fructose (hexokinase can metabolise fructose but has a lower affinity and capacity, Newsholme & Leech, 1983). The sciatic nerve is of particular interest with regard to fructose metabolism as it has the ability to produce fructose from glucose via the polyol pathway, reactions involving aldose reductose and sorbitol dehydrogenase in Schwann cells, a feature shared with liver, ovaries, sperm and seminal vesicles (Champe & Harvey, 2008). An intriguing report in hippocampus demonstrated that the support afforded hippocampal neurones from fructose is mediated via glial cell conversion of fructose to lactate, which is subsequently shuttled to neurones (Izumi & Zorumski, 2009). The sciatic nerve receives its blood supply via the vasa nervosum, where any dietary derived fructose would be available to the nerve In our recording setup, where we record from *in vitro* sciatic nerve, the blood supply is circumvented thus the vasa nervosum would play no role in the supply of fructose to the nerve.

The results presented in this paper provide evidence for the model of substrate use illustrated in Fig 12, and may be summarised as follows. Both A and C fibre conduction is maintained for extended periods in 10 mM glucose, each fibre sub-type directly taking up glucose, although the steady level of [lac] recorded under such conditions implies a tonic lactate efflux from Schwann cells. The inability of cinnemate to block conduction, particularly during CAP recovery experiments, implies no lactate is taken up by either fibre sub-type when supplied with 10 mM glucose, and that cinnemate is not blocking pyruvate uptake into the mitochondria, which would result in a fall in the CAP (Fig 12A). In the absence of exogenously supplied energy substrate, Schwann cell glycogen is metabolised to lactate, which is shuttled to A fibres; the C fibres do not benefit (Fig 12B). Fructose at high concentrations (20 mM) supports the A and C fibre CAPs, but the use of cinnemate reveals profound differences between the two fibres. Cinnemate prevents the ability of 20 mM fructose to maintain or recover the A fibre CAP, and results in a slow, steady increase in [lac], supporting the existence of a shunt in which fructose is converted to lactate in the Schwann cells, and exported for A fibre uptake (Fig 12C). The similarity between the A fibre CAP maintenance with 10 mM fructose in the presence or absence of cinnemate implies the

A fibres do not benefit from this lower concentration of fructose, and that under these conditions Schwann cell glycogen is metabolised to temporarily support conduction (Fig 12D). The C fibres most likely take up fructose directly, although its effectiveness in supporting conduction is impaired by cinnemate. However the following should be borne in mind; the considerable difference in the metabolic demand between small unmyelinated, and larger myelinated axons (Wang *et al.*, 2008), coupled with the relative paucity of information regarding peripheral nerve metabolism, make it possible that at least part of cinnemate's action results from its ability to block mitochondrial pyruvate uptake (McCommis & Finck, 2015). Alternatively, the fall in C fibre CAP may be an indirect result of A fibre loss of function, and the inevitable elevation in interstitial K^+, which is supported by the data shown in Fig 6, where a fall in A fibre CAP in 10 mM or 5 mM fructose is mirrored by a delayed fall in C fibre CAP under equivalent conditions. We are currently using immunohistochemical techniques to explore the cell specific expression of glucose transporters and fructokinase in sciatic nerve.

Lactate shuttle

We can draw two broad conclusions from our data. Firstly, that fibre sub-types present in the sciatic nerve exhibit unique metabolic profiles. This should not be considered surprising given the radically different morphology that exists between myelinated and unmyelinated fibres (Berthold & Rydmark, 1995; Nicholls *et al.*, 2012), which inevitably confer unique metabolic demands on each fibre sub-type, based principally upon the consequences of ion channel distribution (Ritchie, 1995), and the emerging metabolic roles purported for myelinating cells (Lee *et al.*, 2012; Morrison *et al.*, 2015). Whereas Schwann cells ensheath single myelinated fibres in peripheral nerves, the unmyelinated C fibres are grouped within Schwann cell cytoplasm in Remak bundles (Berthold, 1978). Any metabolic role provided by Remak cells is unknown, but it is illuminating to examine the images in Fig 2 to realise the proximity of the C fibres to the interstitial fluid, separated only by a thin basement membrane; some C fibres are exposed directly to the interstitial space (Fig 2F illustrates two such examples). Under such circumstances the relative ease with which fructose may gain access to the C fibres can be readily appreciated. Secondly, that there exists in sciatic nerve lactate shuttling, as previously demonstrated in central tissue. Shuttling of lactate was first proposed to occur in central grey matter (Pellerin & Magistretti, 1994), but has been extended to encompass white matter (Brown *et al.*, 2003) and sciatic

nerve (Brown *et al.*, 2012). Thus, lactate shuttling may be considered a universal process that occurs throughout the nervous system and involves conversion in glia of glucose or glycogen to lactate. The lactate, a metabolic conduit, is subsequently transported, via the interstitial fluid, to neuronal elements to support conduction. As such [lac] recorded in the interstitial space (Suzuki *et al.*, 2011; Brown *et al.*, 2012; Choi *et al.*, 2012; Yang *et al.*, 2014) is a 'substrate in transit' rather than a waste product. The differences between shuttling in the peripheral versus central nervous system must be considered. The brain is protected by the blood brain barrier (Bradbury, 1979), which excludes substances present in the systemic circulation, although transport mechanisms exist for uptake of desirable compounds such as glucose and essential amino acids (Ransom, 2009). The peripheral nerves have no such barrier, but are enclosed within the epineurium and each fibre bundle is further enclosed within the perineurium (King, 1999). These do not offer the same barrier to substrate transport and may be considered leaky. As such systemic substances have relatively easier access to peripheral tissue than the CNS, thus dietary fructose may be a viable substrate for peripheral nerve, whereas its utility in the brain is questionable. The shuttling of fructose to lactate in Schwann cells is novel, but a similar process has been described in hippocampus (Izumi & Zorumski, 2009). We are confident that the Schwann cells produce the lactate for the following reasons. There have been no previous instances of axonal lactate production or export, whereas astrocytes, oligodendrocytes and Schwann cells in culture have all demonstrated this feature. Cinnemate blocks CAP conduction, which, if the lactate were produced by the axons, would lead to axonal retention of lactate and thus be available for metabolism. Where the sciatic nerve differs from the hippocampus (although see Hwang *et al.*, 2017) is that it is able to create fructose from glucose via the polyol pathway (Champe & Harvey, 2008), which is accelerated in diabetes. Our results imply that the Schwann cell is capable of converting fructose to lactate so this may be the ultimate fate of such fructose; any proposals of its significance are purely conjecture.

We have described a method that enables the simultaneous recording of A and C fibre CAPs from mouse sciatic nerve. Perhaps the most useful aspect of the method is the ability to carry out like-with-like comparisons of A and C fibres under identical experimental conditions, which has previously not been possible. Using this method we have routinely recorded conduction in the nerve for periods of up to 8 hours. This extended duration of recording is sufficient to carry out experiments of the type that have been so successfully employed in studies on central white matter injury, and opens up the possibility that equivalent studies may be carried out on peripheral nerve with similar success. Unravelling the metabolic profile of the sciatic nerve and

revealing fibre sub-type specific utility of substrates may be germane in elucidating the mechanisms underlying diabetic neuropathy and ultimately help in developing clinically effective neuro-protective strategies.

Figure Legends

Figure 1

Dissection and recording from mouse sciatic nerve. A. Dissection of the sciatic nerve from the right hind leg. The mouse is pinned prone to a corkboard. The diagonal dotted lines outline the vertebrae. The nerve is exposed and gently teased from adhesions to surrounding muscle. It is cut as it leaves the spinal cord, and distal to where the sciatic nerve branches into the sural, tibial and peroneal nerves. B. The recording set up in which the sciatic nerve (SN) is placed between two suction electrodes, one for stimulating the nerve, the other for recording the stimulus evoked response.
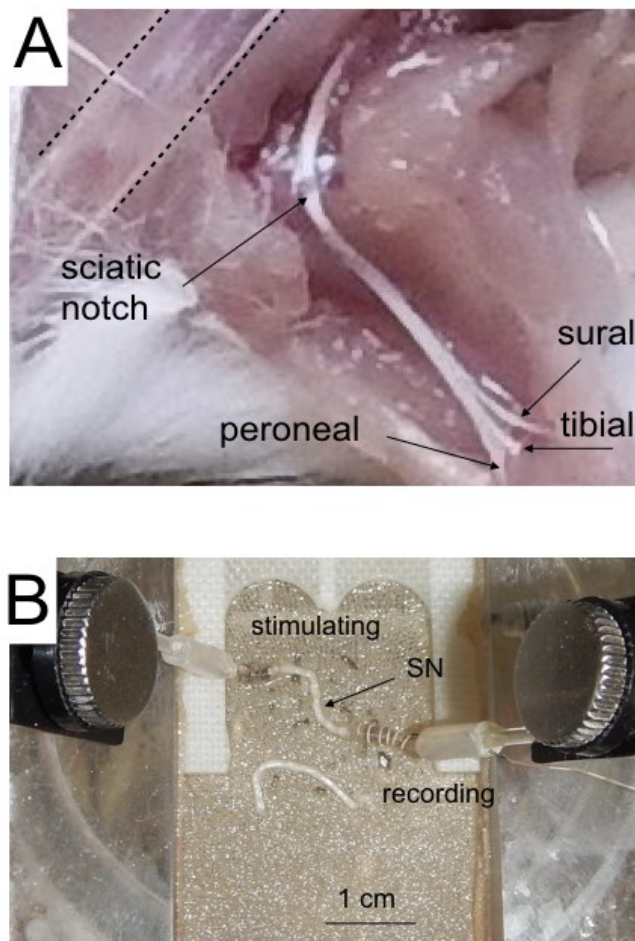
Figure 2

Electron micrographs illustrating the two morphologically distinct fibre sub-types in the mouse sciatic nerve. A. Low power transverse section of sciatic nerve containing large myelinated A fibres (A) and smaller unmyelinated C fibres (C) arranged within Remak bundles. B. Higher power image that allows comparison of the diameter of the unmyelinated C fibres and myelinated A fibres. C. Higher power image of myelinated A fibre showing axoplasm (ax) surrounded by myelin (myl). The Schwann cell nucleus (nuc) and cytoplasm (cyt) are visible in this particular image. A large interstitial space (is) separates the fibres. D. Remak bundle with centrally located nucleus surrounded by C fibres. E. High power image of a Remak bundle containing 13 similarly sized unmyelinated C fibres. F. High power image of individual C fibres contained within Remak bundles. The individual fibres (c) are encased within Schwann cell cytoplasm, which also contain mitochondria (m), and the group of axons enclosed by the basement membrane (bm). Numerous collagen (col) molecules are present in the interstitial space.
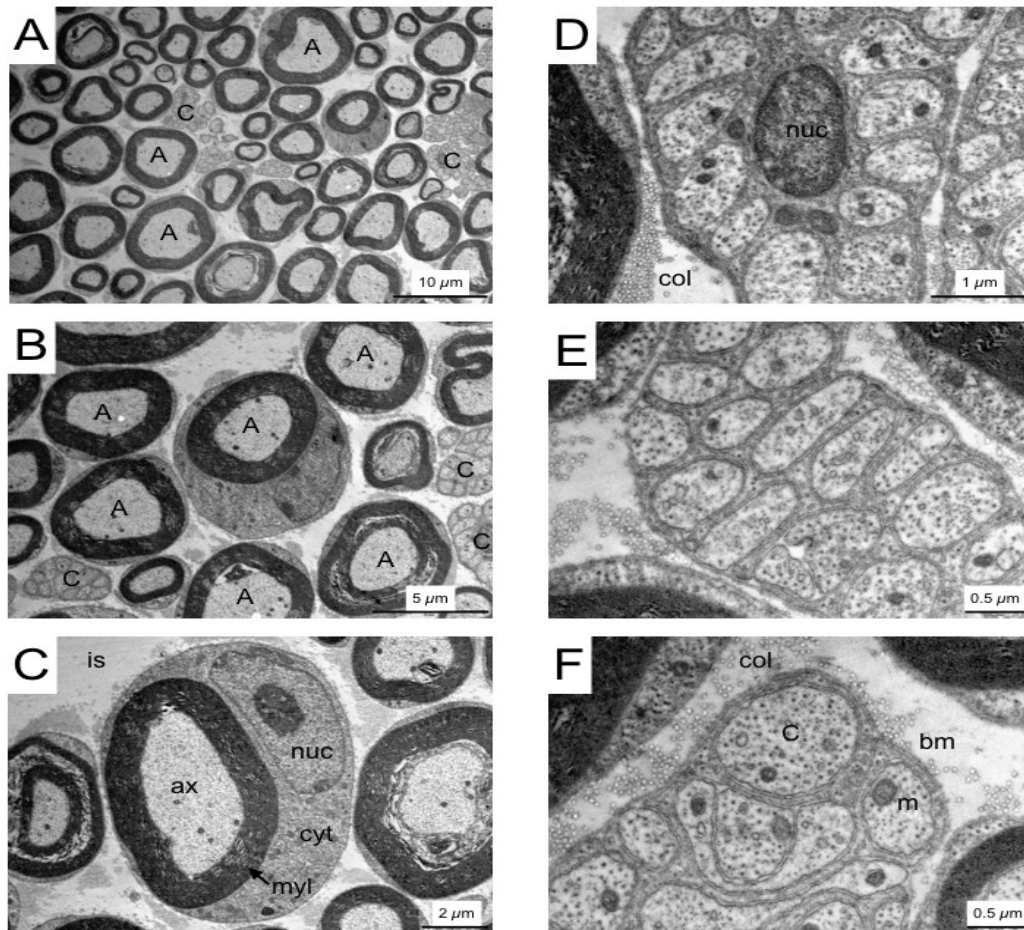
Figure 3

      CAP recorded from sciatic nerve using a paired pulse protocol. A. The 1st stimulus evoked the A fibres, with the C fibres evoked 20 ms later. Note that the C fibre CAP occurs between about 10 and 20 ms after the stimulus, an indication of the slow conduction velocity of the contributing small unmyelinated axons. The A fibre CAP (A) arises soon after the stimulus (* denotes the artefact), whereas the C fibre CAP arises later (C) and its duration exceeds that of the A peak. B. A trace showing the C fibre CAP relative to the background noise (i). Averaging 60 traces, stimulus 1 Hz, vastly improves the signal to noise and permits easy identification of the C fibre CAP (ii). C. The A fibre CAP evoked by a 10 V stimulus (i). Crushing the nerve removes the active response leaving only the stimulus artefact (ii). Subtraction of the stimulus artefact reveals the A fibre CAP. Arrow denotes the peak A fibre CAP amplitude. D. The C fibre CAP evoked by a 150 V stimulus, an averaged response from 60 traces (i). The stimulus artefact as described above (ii), where subtraction removes the majority of the artefact, although some residual remains (*: iii). Arrow denotes the peak C fibre CAP amplitude and the area of the C fibre CAP is shaded.
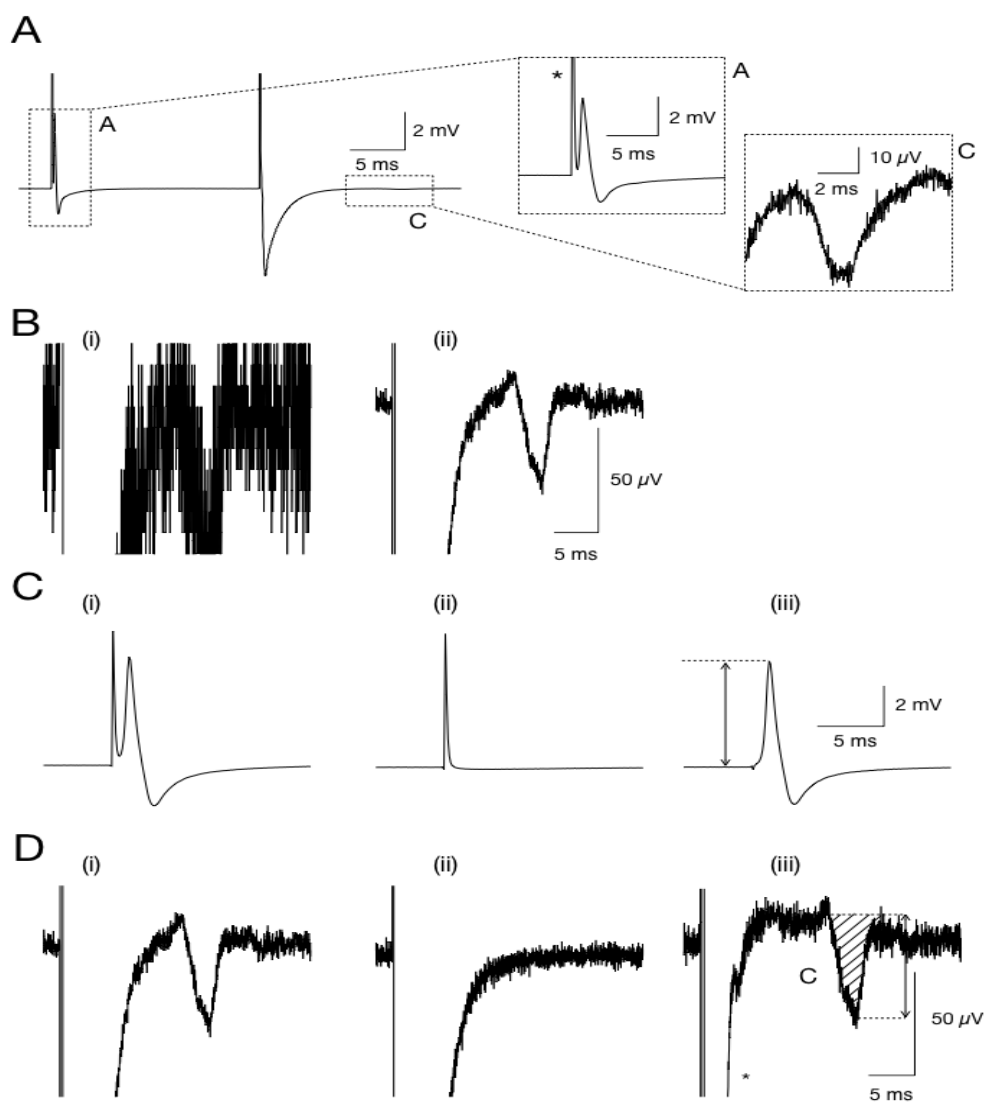
Figure 4

Characteristics of the A and C fibre CAPs. A. Stimulus response plots for A and C fibre CAPs showing that the maximal A fibre CAP occurs below the threshold for C fibre recruitment. The plots were fitted with a Boltzmann sigmoidal relationship with $V_{0.5}$ of 5.3 and 83.7 V, and slope 0.63 and 9.75, respectively, for the A and C fibre CAPs, respectively. B. The amplitude for maximal A fibre CAP was 4.23 ± 1.09 mV (n = 8) versus 92.3 ± 33.3 µV (n = 8) for the C fibre CAP. C. Superimposed A fibre CAPs evoked by a double pulse protocol with the 2nd pulse (P2) occurring at decreased inter-pulse intervals from the 1st (P1). D. The ratio of P2/P1 plotted against the inter-pulse interval shows a decreased P2 peak when the inter-pulse interval is below about 4 ms.
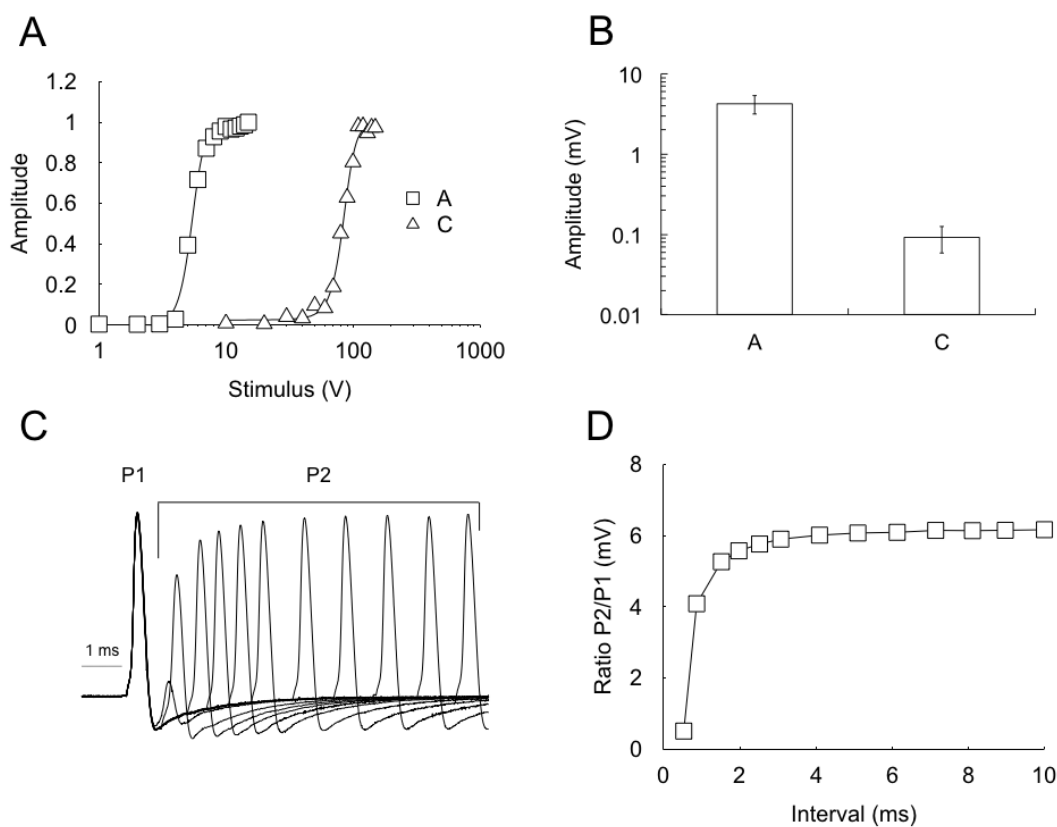

Figure 5

Ability of substrates to support A and C fibre conduction. Switching from control aCSF (10 G), to, in sequence, substrate-free (SF), 10 mM fructose (10 F), 10 mM glucose (10

G) then 10 mM fructose (10 F) revealed the ability of the substrates to support conduction in the A and C fibres, which provides key physiological insights into the metabolic profile of each fibre sub-type. CAPs are expressed as offset normalised amplitudes / areas to allow for optimal comparison between fibre sub-types.
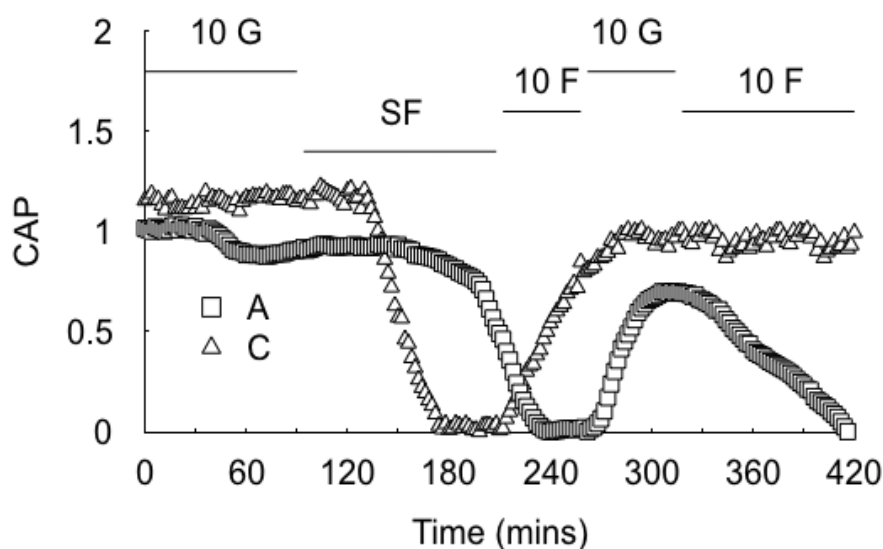

Figure 6

Ability of fructose to maintain the A and C fibre CAPs. A. In substrate free aCSF the CAP fell after about 90 minutes, a latency that was accelerated when 50 Hz stimulus was simultaneously imposed. The CAP was fully supported in 10 mM glucose and 20 mM fructose, but it was not supported in 10 mM fructose or 5 mM fructose. B. The C fibre CAP was more robust that the A fibre, being fully supported in 10 mM glucose and 20 mM fructose, with partial failure occurring with 10 mM or 5 mM fructose aCSF. C. The ability of fructose to support the A and C fibre CAPs was reflected in our measure of CAP maintenance. The A fibre CAP was supported for 475.0 ± 17.2 CAP.mins (n = 5), 465.7 ± 16.4 CAP.mins (n = 3), 249.3 ± 115.9 CAP.mins (n = 6), 201.5 ± 82.5 CAP.mins (n = 4), 151.2 ± 27.5 (n = 4) or 75 ± 12.7 (n = 3), respectively, in 10 mM glucose, 20 mM fructose, 10 mM fructose, 5 mM fructose, substrate free aCSF or imposition of 50 Hz, respectively. The C fibre

CAP was supported for 467.3 ± 14.3 CAP.mins (n = 3), 476.5 ± 5.6 CAP.mins (n = 2), 409.2 ± 3.2 CAP.mins (n = 3), 393.1 ± 9.3 CAP.mins (n = 3) or 63.5 ± 4.4 CAP.mins (n = 4), respectively in 10 mM glucose, 20 mM fructose, 10 mM fructose, 5 mM fructose or substrate free aCSF, respectively. One-way ANOVA with Sidak post-test. ns = not significant, *** p < 0.0005, **** p < 0.0001.

Figure 7

Effects of fructose pre-incubation on latency to A fibre CAP failure. A. Pre-incubating the sciatic nerves in aCSF containing 10 mM fructose for 2 hours accelerated CAP failure on subsequent exposure to substrate-free aCSF compared to nerves pre-incubated in either 10 mM glucose or 20 mM fructose. B. Exposure to 10 mM fructose aCSF for 2 hours significantly decreased A fibre CAP maintenance during subsequent exposure to substrate free aCSF (61.2 ± 17.7 CAP.mins: n = 4) compared to nerves pre-incubated in either 10 mM glucose (151.3 ± 27.7 CAP.mins: n = 4) or 20 mM fructose (155.6 ± 9.8 CAP.mins: n = 5). One-way ANOVA with Sidak post-test. ns = not significant, **** $p < 0.0001$.
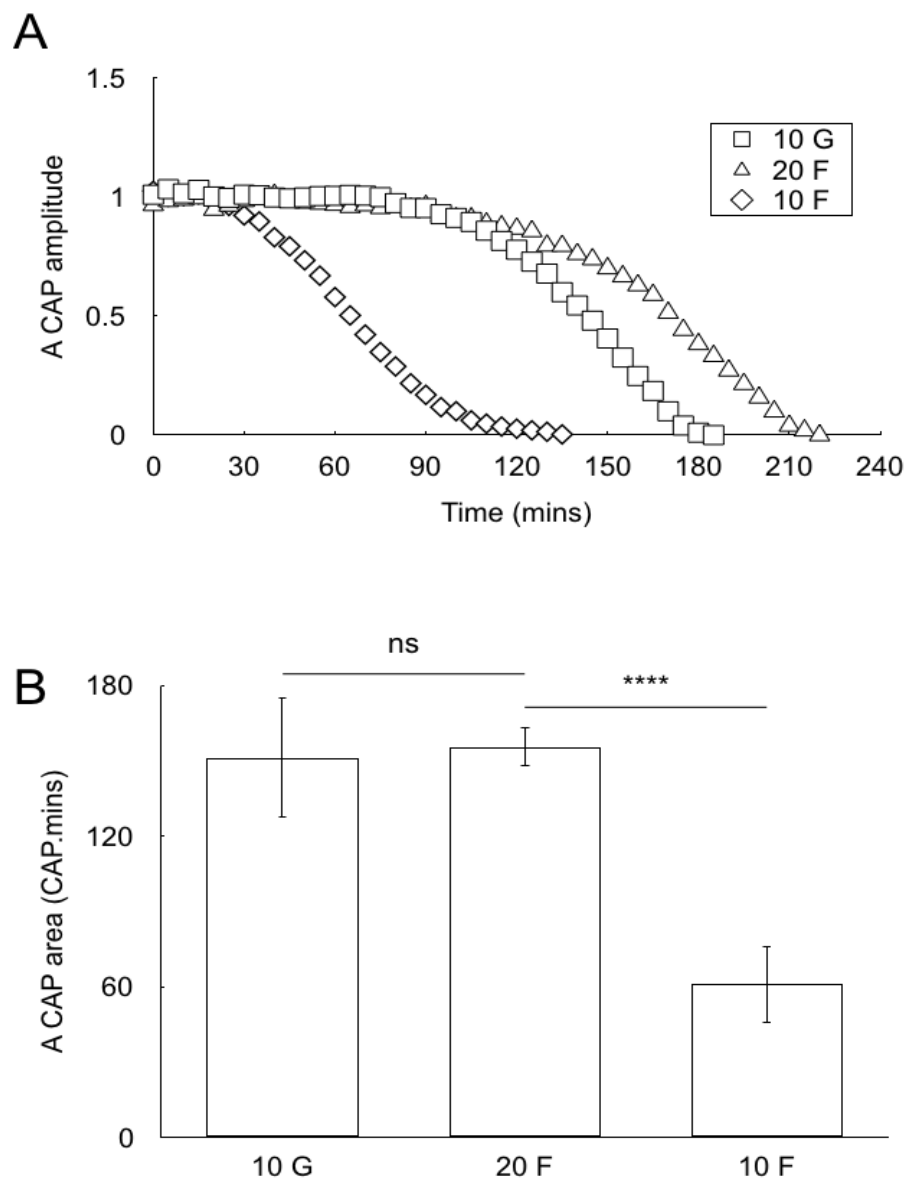
Figure 8

Ability of fructose to recover A and C fibre CAPs. A. Exposure to substrate-free (SF) aCSF was used to deplete glycogen and induce A fibre CAP failure. Subsequent exposure to 10 mM glucose (10 G) resulted in rapid CAP recovery, whereas 20 mM fructose (20 F) resulted in delayed CAP recovery and 10 mM fructose (10 F) failed to recover the CAP. In nerves that failed to recover on exposure to 10 mM fructose, subsequent exposure to 10 mM glucose (lower horizontal line) led to partial CAP recovery. B. The C fibre CAP recovered rapidly and completely in 10 mM glucose, 20 mM fructose or 10 M fructose. C. The A fibre CAP recovery was 98.7 ± 1.9 % (n = 6), 87.7 ± 11.2 % (n = 3) or 0 ± 0 % (n = 4), respectively, whereas the C fibre recovery was 92.1 ± 8.8 % (n = 3), 99.9 ± 0.1% (n = 3) or 93.8 ± 7.4 % (n = 3), respectively, in 10 mM glucose, 20 mM fructose or 10 mM fructose, respectively. D. The recovery time, the time taken for the CAP to recover to its amplitude at the end of the period of substrate-free aCSF exposure, was 7.1 ± 4.4 minutes (n = 6) and 35.7 ± 15.9 minutes (n = 3) for A fibres in 10 mM glucose or 20 mM fructose, respectively: there is no value for 10 mM fructose where the CAP did not recover. For the C fibre CAP recovery time was 1.3 ± 0.6 minutes (n = 3), 1.7 ± 1.1 minutes (n = 3) or 5.7 ± 5.0 minutes (n = 3) for nerves recovered in 10 mM glucose, 20 mM fructose or 10 mM fructose. One-way ANOVA with Sidak post-test. ns = not significant, ** $p < 0.005$, **** $p < 0.0001$.
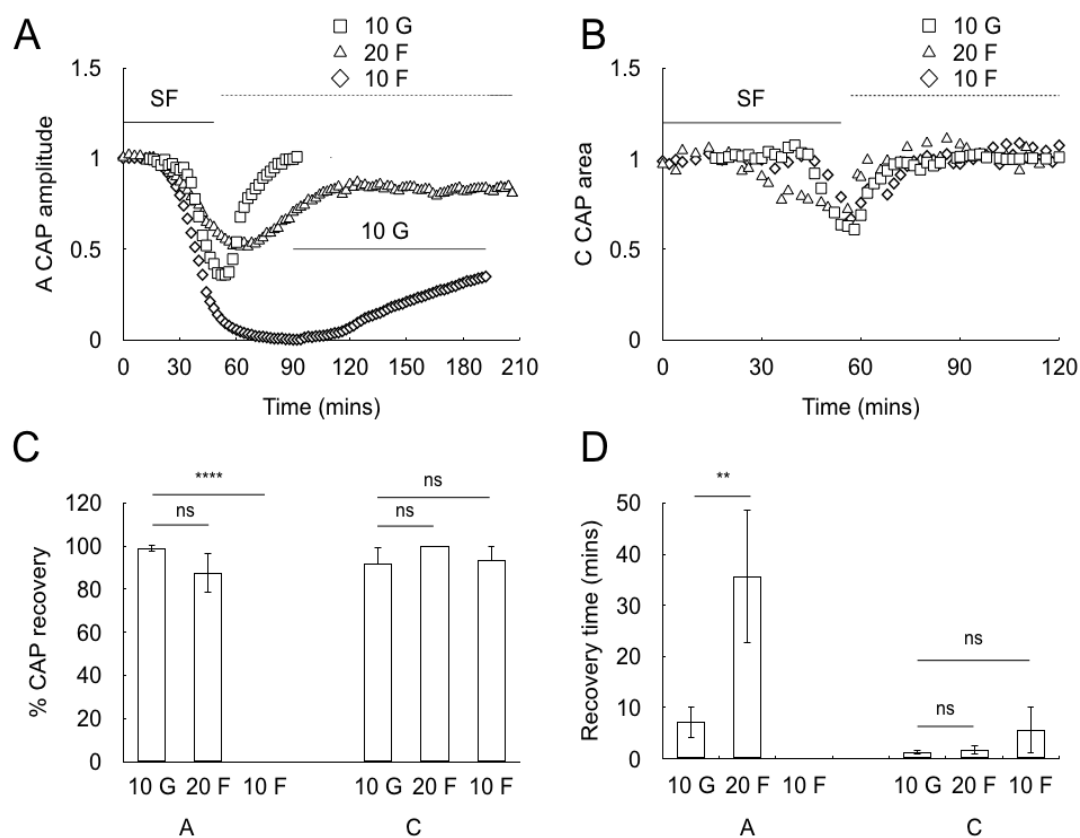
Figure 9

Ability of fructose to support the A and C fibre CAPs in the presence of cinnemate. A. The A fibre CAP was fully maintained in control aCSF plus cinnemate (10 G + CIN), but in 20 mM fructose (20 F + CIN) or 10 mM fructose (10 F + CIN) plus cinnemate the CAP fell with a latency akin to that of nerves exposed to substrate-free aCSF (SF). B. The C fibre CAP was fully maintained in control aCSF plus cinnemate and in 20 mM fructose plus cinnemate, but partially failed in 10 mM fructose plus cinnemate, although CAP maintenance was greater than in nerves exposed to substrate free aCSF. C. The A fibre CAP was supported for 475.0 ± 17.2 CAP.mins (n = 5), 488.5 ± 18.4 CAP.mins (n = 3), 465.7 ± 16.4 CAP.mins (n = 3), 220.7 ± 96.1 CAP.mins (n = 6), 249.3 ± 115.9 CAP.mins (n = 6), 215.9 ± 55.0 (n = 5) or 151.3 ± 27.7 CAP.mins (n = 4), respectively in 10 mM glucose, 10 mM glucose plus cinnemate, 20 mM fructose, 20 mM fructose plus cinnemate, 10 mM fructose, 10 mM fructose plus cinnemate or substrate free aCSF, respectively. D. The C fibre CAP was supported for 475.4 ± 3.7 CAP.mins (n = 2), 483.4 ± 0.7 CAP.mins (n = 2), 476.5 ± 5.6 CAP.mins (n = 2), 488.0 ± 10.9 CAP.mins (n = 2), 409.2 ± 3.2 CAP.mins (n = 3), 266.3 ± 12.5 (n = 3) or 63.5 ± 4.4 CAP.mins (n = 4), respectively in 10 mM glucose, 10 mM glucose plus cinnemate, 20 mM fructose, 20 mM glucose plus cinnemate, 10 mM fructose, 10 mM fructose plus cinnemate or substrate free aCSF, respectively. One-way ANOVA with Sidak post-test. ns = not significant, *** $p < 0.0005$, **** $p < 0.0001$.
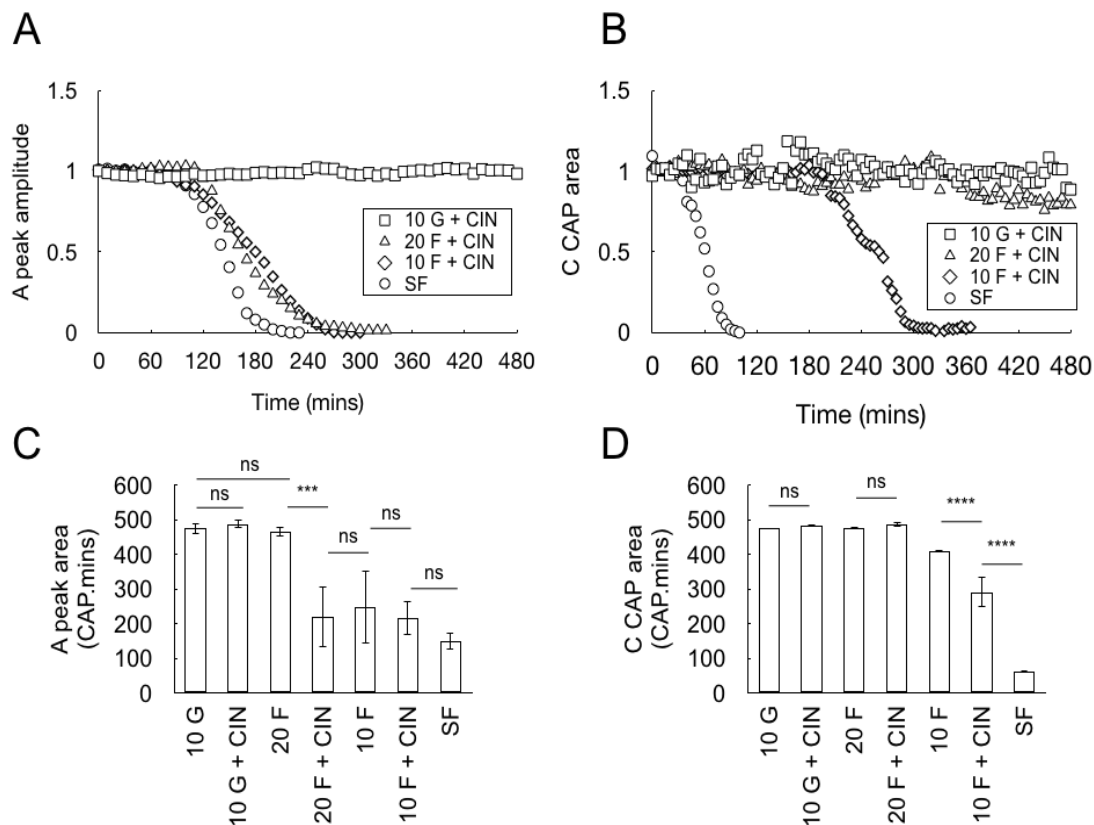
Figure 10

Ability of fructose to recover A and C fibre CAPs in the presence of cinnemate. A. Exposure of nerves to substrate-free aCSF (SF) caused A fibre failure which was recovered by subsequent introduction of control aCSF plus cinnemate (10 G + CIN). B. aCSF containing 20 mM fructose plus cinnemate (20 F + CIN) was unable to recover the CAP. The stark contrast between the efficacy of glucose and fructose is clearly seen where control aCSF plus cinnemate (10 G + CIN) recovers the CAP, which then falls on subsequent introduction of 20 mM fructose plus cinnemate. C. Both 10 mM glucose plus cinnemate and 20 mM fructose plus cinnemate fully recover the C fibre CAP. D. The A fibre CAP recovery was 98.7 ± 1.9 % (n = 6), 92.5 ± 6.8 % (n = 3), 87.7 ± 11.2 (n = 3) or 0 ± 0 % (n = 3), respectively, whereas the C fibre recovery was 92.1 ± 8.8% (n = 3), 94.3 ± 8.3 % (n = 3), 99.9 ± 0.1 % (n = 3) or 95.1 ± 6.9 % (n = 2), respectively, in 10 mM glucose, 10 mM glucose plus cinnemate, 20 mM fructose or 20 mM fructose plus cinnemate, respectively. One-way ANOVA with Sidak post-test. ns = not significant, **** p < 0.0001.
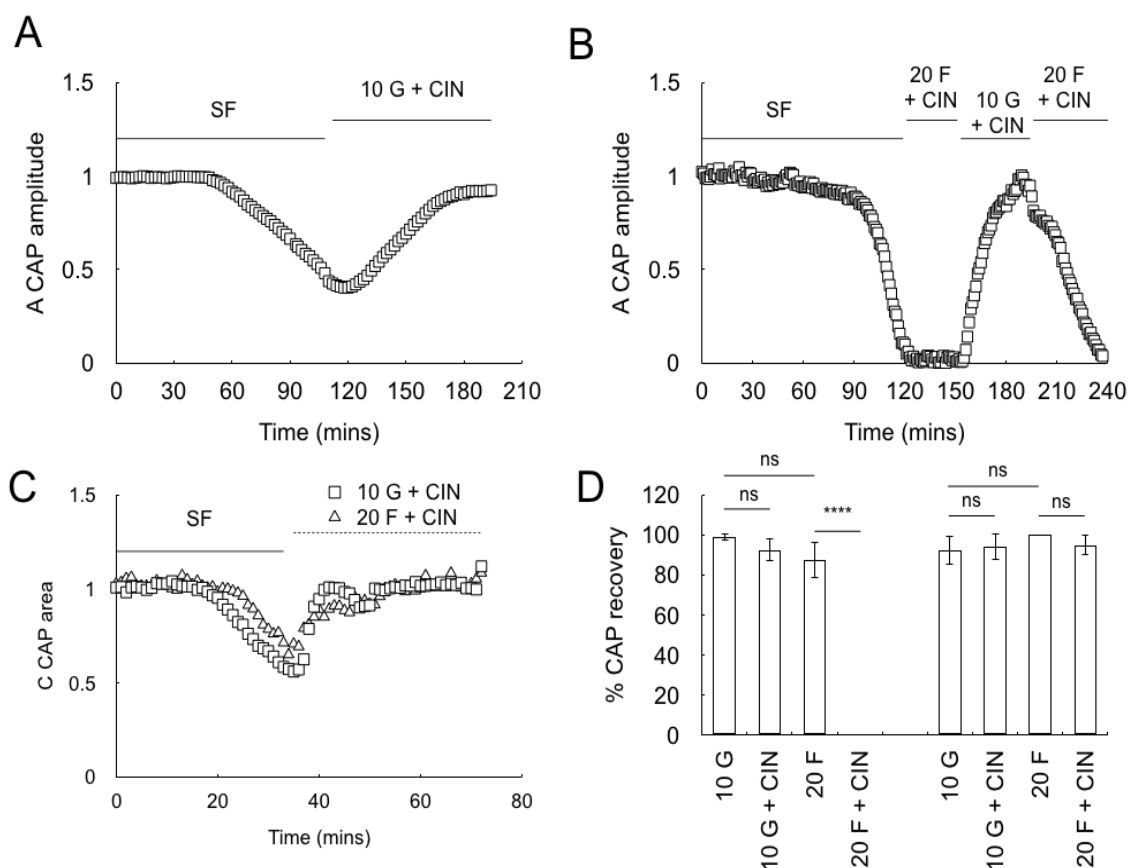
Figure 11

Lactate flux in sciatic nerve. A. A [lac] dose response relationship in the presence of varying [glucose] (n = 5). B. In sciatic nerves exposed to control aCSF (10 G) the [lac] is steady at about 50 μM. Introducing 20 mM fructose aCSF (20 F) causes a fall in [lac] to a new steady value of about 15 μM. However in 10 mM fructose (10 F) there was a fall in [lac] to zero (n = 3). C. Recovery of the A fibre CAP with in 20 mM fructose is delayed compared to recovery in 10 mM glucose. There is a temporal correlation between the onset of CAP recovery and the peak [lac] level reached after introduction of 20 mM fructose (see inset, where minor ticks on x-axis are 10 minutes, on the y-axis they are 25 μM, the CAP is scaled for optimal visibility, the vertical dotted line signifies the introduction of 20 mM fructose aCSF; n = 5). D. [Lac] is steady when 20 mM fructose is perfused but slowly and reversibly increases on introduction of 200 μM cinnemate (n = 3).
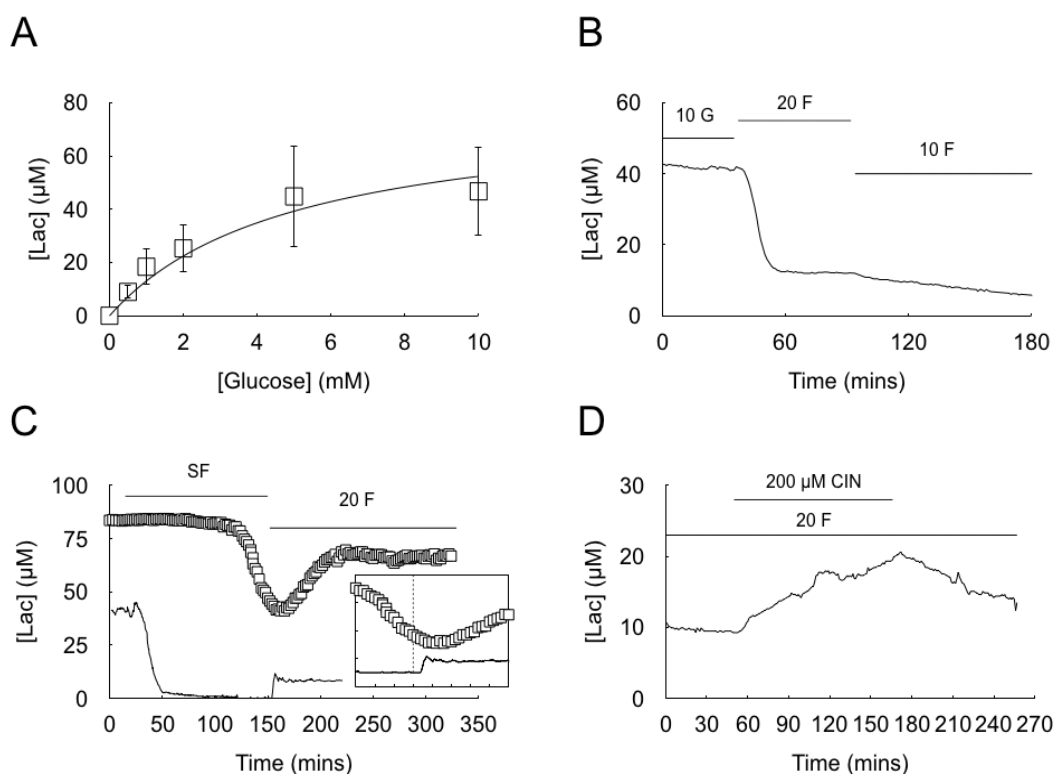
Figure 12

Model comparing substrate pathways during the experimental manoeuvres described in the paper. A. Under normal conditions when nerves were perfused with control aCSF containing 10 mM glucose, the glucose was taken up directly into the A and C fibres, as cinnemate had no effect on the ability of 10 mM glucose (Gluc) to support the A or C fibre CAPs. However lactate (Lac) is tonically released from the Schwann cells (SC) under these conditions as demonstrated by our measurements of a stable [lac]. B. Under aglycemic conditions the Schwann cell glycogen (Glyc) is broken down to lactate which is shuttled to support A fibre conduction. The C fibres receive no benefit from this glycogen. At the onset of aglycemia [lac] falls to zero indicating all lactate is taken up into the A fibres. The filled circle indicates the cinnemate sensitive monocarboxylate transporter, which facilitates fibre uptake of lactate. C. The C fibres directly take up 20 mM fructose (20 F), but it is shuttled to lactate via the Schwann cells, then it is taken up by the A fibres. D. The C fibres directly take up 10 mM fructose (10 F), but it appears to be of little direct benefit to the A fibres, which are supported by metabolism of Schwann cell glycogen until the glycogen is exhausted.
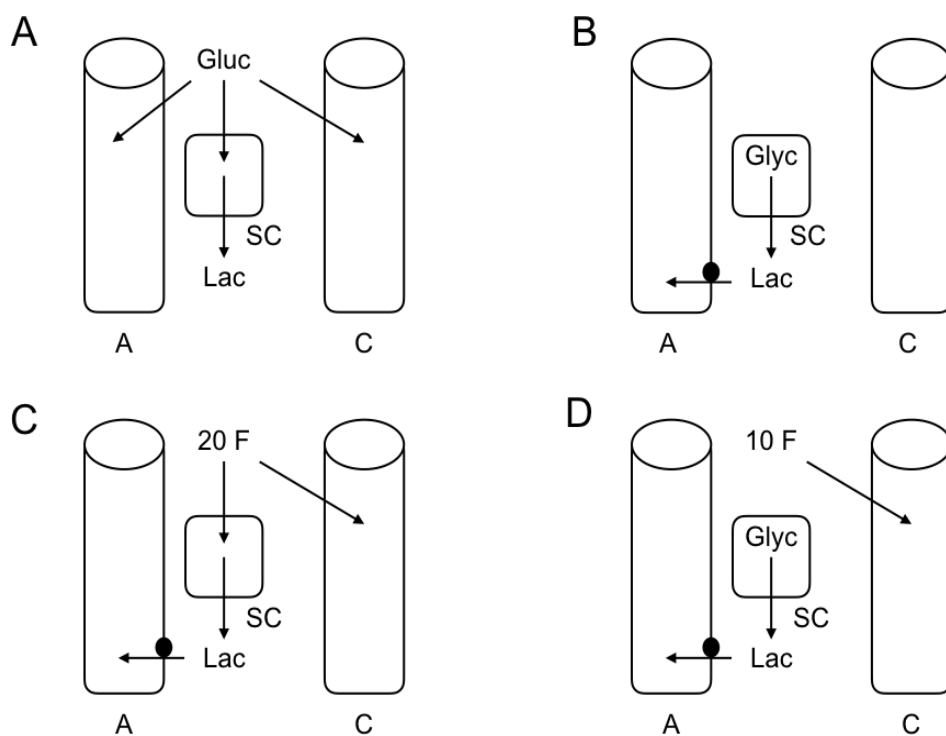
Table 1

Summary of the ability of glucose and varying concentrations of fructose, in the presence or absence of cinnemate, to maintain or recover the A and C fibre CAP. Data are extracted from Fig 6C, Fig 8D, Fig 9C & D and Fig 10D. The measure of the ability of the substrates to maintain the CAP was calculated as the maximum value in 10 mM glucose minus the value in substrate free aCSF. This was then converted to a percentage.. Note that by expressing the 0 mM glucose data as nominally 0 % baseline, the accelerating effect of 50 Hz stimulus on A fibre CAP latency compared to baseline returns a negative value.

Table 1

Substrate	Maintain (%)		Recover (%)	
	A	C	A	C
10 mM glucose	100	100	98.7	92.1
20 mM fructose	96.9	102.2	87.7	99.9
10 mM fructose	30.2	85.6	0	93.8
5 mM fructose	15.4	81.7		
0 mM glucose	0	0		
0 mM glucose + 50 Hz stimulus	-23.4			
10 mM glucose + CIN	104.2	104.1	92.5	94.3
20 mM fructose + CIN	21.5	105.2	0	99.9
10 mM fructose + CIN	20.0	50.3		95.1

References

Alix JJ & Fern R. (2009). Glutamate receptor-mediated ischemic injury of premyelinated central axons. *Ann Neurol* **66,** 682-693.

Allen L, Anderson S, Wender R, Meakin P, Ransom BR, Ray DE & Brown AM. (2006). Fructose supports energy metabolism of some, but not all, axons in adult mouse optic nerve. *J Neurophysiol* **95,** 1917-1925.

Allen NJ, Karadottir R & Attwell D. (2005). A preferential role for glycolysis in preventing the anoxic depolarization of rat hippocampal area CA1 pyramidal cells. *J Neurosci* **25,** 848-859.

Baltan S, Besancon EF, Mbow B, Ye Z, Hamner MA & Ransom BR. (2008). White matter vulnerability to ischemic injury increases with age because of enhanced excitotoxicity. *J Neurosci* **28,** 1479-1489.

Baltan Tekkök S, Brown AM & Ransom BR. (2003). Axon function persists during anoxia in mammalian white matter. *J Cereb Blood Flow Met* **23,** 1340-1348.

Bernheim F & Bernheim MLC. (1941). Note on the oxidation of various sugars by brain tissue. *J Biol Chem* **140,** 441-444.

Berthold C-H. (1978). Morphology of normal peripheral axons. In *Physiology and Pathology of Axons*, ed. Waxman SG, pp. 3-63. Raven Press, New York.

Berthold C-H & Rydmark M. (1995). Morphology of normal peripheral axons. In *The Axon*, ed. Waxman SG, Kocsis JD & Stys PK, pp. 13-48. Oxford, OUP.

Bradbury MG. (1979). *The concept of the blood brain barrier*. Wiley and Sons, London

Brown AM, Baltan Tekkok S & Ransom BR. (2004). Energy transfer from astrocytes to axons: the role of CNS glycogen. *Neurochem Int* **45,** 529-536.

Brown AM, Evans RD, Black J & Ransom BR. (2012). Schwann cell glycogen selectively supports myelinated axon function. *Ann Neurol* **72,** 406-418.

Brown AM & Rich LR. (2017). An improved method that allows simultaneous recording of stimulus evoked A and C fibre conduction in mouse sciatic nerve. *Proc Physiol Soc* **39**.

Brown AM, Sickmann HM, Fosgerau K, Lund TM, Schousboe A, Waagepetersen HS & Ransom BR. (2005). Astrocyte glycogen metabolism is required for neural activity during aglycemia or intense stimulation in mouse white matter. *J Neurosci Res* **79,** 74-80.

Brown AM, Tekkok SB & Ransom BR. (2003). Glycogen regulation and functional role in mouse white matter. *J Physiol* **549,** 501-512.

Brown AM, Wender R & Ransom BR. (2001a). Ionic mechanisms of aglycemic axon injury in mammalian central white matter. *J Cereb Blood Flow Met* **21,** 385-395.

Brown AM, Wender R & Ransom BR. (2001b). Metabolic substrates other than glucose support axon function in central white matter. *J Neurosci Res* **66,** 839-843.

Champe PC & Harvey RA. (2008). *Biochemistry*. Lippincott Williams & Wilkins, Baltimore.

Choi HB, Gordon GR, Zhou N, Tai C, Rungta RL, Martinez J, Milner TA, Ryu JK, McLarnon JG, Tresguerres M, Levin LR, Buck J & MacVicar BA. (2012). Metabolic communication between astrocytes and neurons via bicarbonate-responsive soluble adenylyl cyclase. *Neuron* **75,** 1094-1104.

Cummins KL, Perkel DH & Dorfman LJ. (1979). Nerve fiber conduction-velocity distributions. I. Estimation based on the single-fiber and compound action potentials. *Electroencephalogr Clin Neurophysiol* **46,** 634-646.

Dalle C, Schneider M, Clergue F, Bretton C & Jirounek P. (2001). Inhibition of the I(h) current in isolated peripheral nerve: a novel mode of peripheral antinociception? *Muscle Nerve* **24,** 254-261.

Devuyst G & Bogousslavsky J. (1999). Clinical trial update: neuroprotection against acute ischaemic stroke. *Curr Opin Neurol* **12,** 73-79.

Dirnagl U, Iadecola C & Moskowitz MA. (1999). Pathobiology of ischaemic stroke: an integrated view. *TiNS* **22,** 391-397.

Docherty RJ, Charlesworth G, Farrag K, Bhattacharjee A & Costa S. (2005). The use of the rat isolated vagus nerve for functional measurements of the effect of drugs in vitro. *J Pharmacol Toxicol Methods* **51,** 235-242.

Erne-Brand F, Jirounek P, Drewe J, Hampl K & Schneider MC. (1999). Mechanism of antinociceptive action of clonidine in nonmyelinated nerve fibres. *Eur J Pharmacol* **383,** 1-8.

Garthwaite G, Brown G, Batchelor AM, Goodwin DA & Garthwaite J. (1999). Mechanisms of ischaemic damage to central white matter axons: a quantitative histological analysis using rat optic nerve. *Neuroscience* **94,** 1219-1230.

Gaumann DM, Brunet PC & Jirounek P. (1992). Clonidine enhances the effects of lidocaine on C-fiber action potential. *Anesth Analg* **74,** 719-725.

Gaumann DM, Brunet PC & Jirounek P. (1994). Hyperpolarizing afterpotentials in C fibers and local anesthetic effects of clonidine and lidocaine. *Pharmacology* **48,** 21-29.

Grundy D. (2015). Principles and standards for reporting animal experiments in The Journal of Physiology and Experimental Physiology. *J Physiol* **593,** 2547-2549.

Harris JJ & Attwell D. (2012). The energetics of CNS white matter. *J Neurosci* **32,** 356-371.

Hodgkin AL. (1954). A note on conduction velocity. *J Physiol* **125,** 221-224.

Hothersall JS, Baquer NZ & McLean P. (1982). Pathways of carbohydrate metabolism in peripheral nervous tissue. I. The contribution of alternative routes of glucose utilization in peripheral nerve and brain. *Enzyme* **27,** 259-267.

Hwang JJ, Jiang L, Hamza M, Dai F, Belfort-DeAguiar R, Cline G, Rothman DL, Mason G & Sherwin RS. (2017). The human brain produces fructose from glucose. *JCI Insight* **2,** e90508.

Izumi Y & Zorumski CF. (2009). Glial-neuronal interactions underlying fructose utilization in rat hippocampal slices. *Neuroscience* **161,** 847-854.

Jirounek P, Bretton C & Dalle C. (2002). Axon-glia interactions modulate axonal excitability in mammalian unmyelinated nerves. *J Physiol Paris* **96,** 237-241.

King RC. (1999). *Atlas of Peripheral Nerve Pathology*. Arnold, London.

Klein R. (1944). Oxidation of fructose by brain in vitro. *J Biol Chem* **153,** 295-300.

Lacomis D. (2002). Small-fiber neuropathy. *Muscle Nerve* **26,** 173-188.

Lee Y, Morrison BM, Li Y, Lengacher S, Farah MH, Hoffman PN, Liu Y, Tsingalia A, Jin L, Zhang PW, Pellerin L, Magistretti PJ & Rothstein JD. (2012). Oligodendroglia metabolically support axons and contribute to neurodegeneration. *Nature* **487,** 443-448.

McCommis KS & Finck BN. (2015). Mitochondrial pyruvate transport: a historical perspective and future research directions. *Biochem J* **466,** 443-454.

McIlwain H. (1953). Substances which support respiration and metabolic response to electrical impulses in human cerebral tissues. *J Neurol Neurosurg Psychiatry* **16,** 257-266.

McIlwain H & Bachelard HS. (1985). *Biochemistry and the Central Nervous System.* Churchill Livingstone, London.

Meakin PJ, Fowler MJ, Rathbone AJ, Allen LM, Ransom BR, Ray DE & Brown AM. (2007). Fructose metabolism in the adult mouse optic nerve, a central white matter tract. *J Cereb Blood Flow Metab* **27,** 86-99.

Mohseni S. (2001). Hypoglycemic neuropathy. *Acta Neuropathol (Berl)* **102,** 413-421.

Morrison BM, Tsingalia A, Vidensky S, Lee Y, Jin L, Farah MH, Lengacher S, Magistretti PJ, Pellerin L & Rothstein JD. (2015). Deficiency in monocarboxylate transporter 1 (MCT1) in mice delays regeneration of peripheral nerves following sciatic nerve crush. *Exp Neurol* **263,** 325-338.

Navarro X, Kennedy WR & Fries TJ. (1989). Small nerve fiber dysfunction in diabetic neuropathy. *Muscle Nerve* **12,** 498-507.

Nave KA. (2010). Myelination and support of axonal integrity by glia. *Nature* **468,** 244-252.

Newsholme EA & Leech AR. (1983). *Biochemistry for the Medical Sciences*. John Wiley and Sons, New York.

Nicholls JG, Martin AR, Fuchs PA, Brown DA, Diamond ME & Weisblat DA. (2012). Electrical Signaling in Neurons. In *From Neuron to Brain*, 5th edn, ed. Nicholls JG,

Martin AR, Fuchs PA, Brown DA, Diamond ME & Weisblat DA, pp. 129-142. Sinauer Associates, Inc, Sunderland, MA, USA.

Ozaki K, Sano T, Tsuji N, Matsuura T & Narama I. (2010). Insulin-induced hypoglycemic peripheral motor neuropathy in spontaneously diabetic WBN/Kob rats. *Comp Med* **60,** 282-287.

Patton HD. (1982). Special properties of nerve trunks and tracts. In *Physiology and Biophysics: IV Excitable Tissues and Reflex Control of Muscle*, ed. Ruch T & Patton H, pp. 101-127. W.B. Saunders Company, Philadelphia.

Pellerin L, Bouzier-Sore AK, Aubert A, Serres S, Merle M, Costalat R & Magistretti PJ. (2007). Activity-dependent regulation of energy metabolism by astrocytes: an update. *Glia* **55,** 1251-1262.

Pellerin L & Magistretti PJ. (1994). Glutamate uptake into astrocytes stimulates aerobic glycolysis: a mechanism coupling neuronal activity to glucose utilization. *Proc Natl Acad Sci USA* **91,** 10625-10629.

Ransom B. (2009). The neuronal microenvironment. In *Medical Physiology*, ed. Boron WF & Boulpaep EL, pp. 289-309. Saunders Elsevier, Philadelphia.

Ritchie JM. (1995). Physiology of axons. In *The Axon*, ed. Waxman SG, Kocsis JD & Stys PK, pp. 68-96. OUP, Oxford.

Rushton WA. (1951). A theory of the effects of fibre size in medullated nerve. *J Physiol* **115,** 101-122.

Salter MG & Fern R. (2008). The mechanisms of acute ischemic injury in the cell processes of developing white matter astrocytes. *J Cereb Blood Flow Metab* **28,** 588-601.

Stecker MM & Stevenson M. (2014). Effect of glucose concentration on peripheral nerve and its response to anoxia. *Muscle Nerve* **49,** 370-377.

Stecker MM & Stevenson MR. (2015). Anoxia-induced changes in optimal substrate for peripheral nerve. *Neuroscience* **284,** 653-667.

Stys PK, Ransom BR & Waxman SG. (1991). Compound action potential of nerve recorded by suction electrode: a theoretical and experimental analysis. *Brain Res* **546,** 18-32.

Stys PK, Waxman SG & Ransom BR. (1992). Ionic mechanisms of anoxic injury in mammalian CNS white matter: role of Na^+ channels and Na^+-Ca^{2+} exchanger. *J Neurosci* **12,** 430-439.

Suzuki A, Stern SA, Bozdagi O, Huntley GW, Walker RH, Magistretti PJ & Alberini CM. (2011). Astrocyte-neuron lactate transport is required for long-term memory formation. *Cell* **144,** 810-823.

Tomlinson DR & Gardiner NJ. (2008). Glucose neurotoxicity. *Nat Rev Neurosci* **9,** 36-45.

Velumian AA, Wan Y, Samoilova M & Fehlings MG. (2010). Modular double sucrose gap apparatus for improved recording of compound action potentials from rat and mouse spinal cord white matter preparations. *J Neurosci Meth* **187,** 33-40.

Wang SS, Shultz JR, Burish MJ, Harrison KH, Hof PR, Towns LC, Wagers MW & Wyatt KD. (2008). Shaping of white matter composition by biophysical scaling constraints. *J Neurosci* **28,** 4047-4056.

Waxman SG & Bennett MV. (1972). Relative conduction velocities of small myelinated and non-myelinated fibres in the central nervous system. *Nat New Biol* **238,** 217-219.

WinWCP. http://spider.science.strath.ac.uk/sipbs/software_ses.htm).

Accepted Article

Yang X, Hamner MA, Brown AM, Evans RD, Ye ZC, Chen S & Ransom BR. (2014). Novel hypoglycemic injury mechanism: N-methyl-D-aspartate receptor-mediated white matter damage. *Ann Neurol* **75,** 492-507.

Author Contribution

AMB was responsible for the conception and design of the study, LRR carried out all the electrophysiology studies, AMB and LRR carried out the lactate sensor studies, LRR analysed the data, AMB wrote the paper with input from LRR. Both authors approved the final version of the work submitted for publication and agree to be accountable for all aspects of this work.